Supporting Information

Green and Controllable Synthesis of Large-Scale High-Quality Two-Dimensional Boron Nitride by Ambient-Pressure Chemical Vapor Deposition

Yi-Lun Hong*, Ci Kong, Jihang Xuan, Yi Zheng, Yuebin Lian, Pinyun Ren*

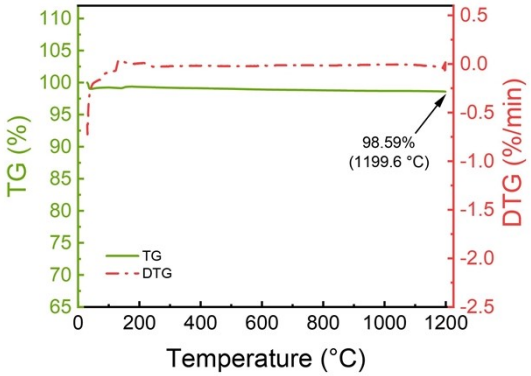

Figure S1. Thermo-gravimetric test of the h-BN powder in pure Ar atmosphere with ramp rate of 20 °C/min.

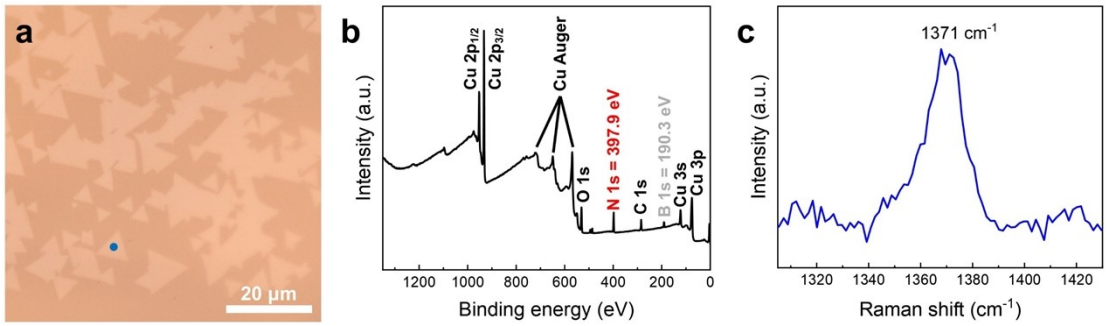

Figure S2. a) An optical image of 2D h-BN samples grown on a Cu substrate with cubic BN (c-BN) powders. b) Survey XPS spectra of 2D h-BN samples grown on a Cu substrate in (a). The peaks of B 1s and N 1s are consistent with those of 2D h-BN samples grown with h-BN powders, which are mentioned later. c) Raman spectra of a

2D h-BN domain (blue spot in (a)), which confirming monolayer h-BN.

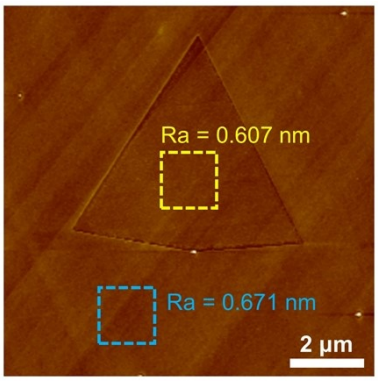

Figure S3. An AFM image of a monolayer h-BN sample grown on a Cu substrate before transfer. This monolayer h-BN sample consists of two crystal domains and the grain boundary between them is smooth and seamless. The surface roughness of this monolayer h-BN sample is smoother than that of Cu substrate used in the growth process.

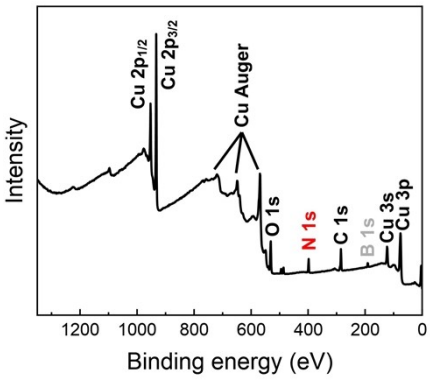

Figure S4. Survey XPS spectra of 2D h-BN samples grown on a Cu substrate by using h-BN powders in Figure 1e.

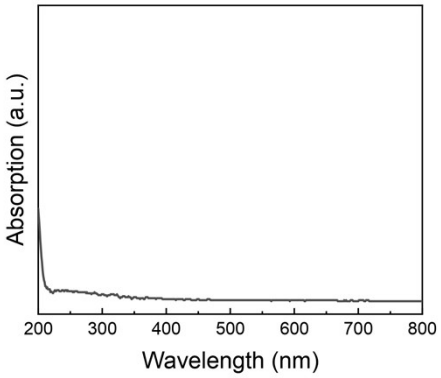

Figure S5. The UV-visible absorption spectrum of a monolayer h-BN film transferred onto a quartz substrate. The corresponding OBG analysis is shown in Figure 1f.

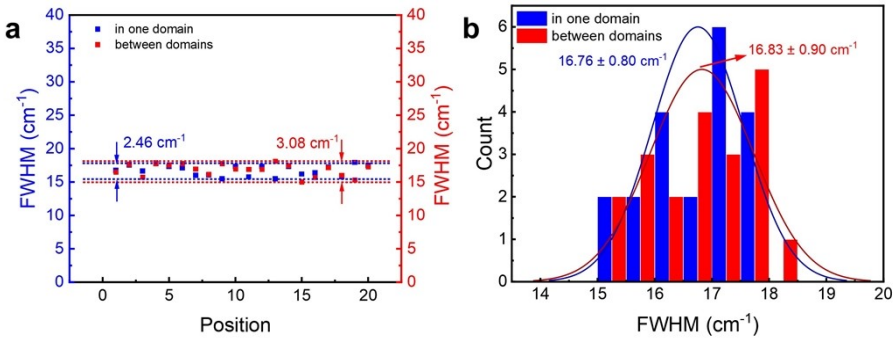

Figure S6. a) The offset of FWHM of 20 E_{2g} peaks both in one domain and between domains. b) Histograms of FWHM of 20 E_{2g} peaks both in one domain and between domains.

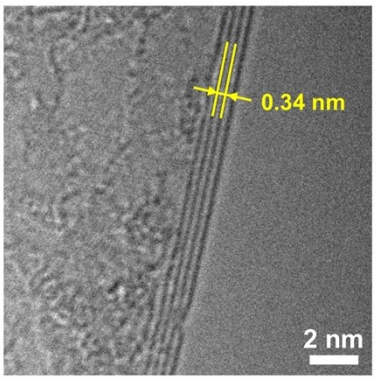

Figure S7. HRTEM image of a folded edge of a few-layer h-BN sample transferred on a TEM grid.

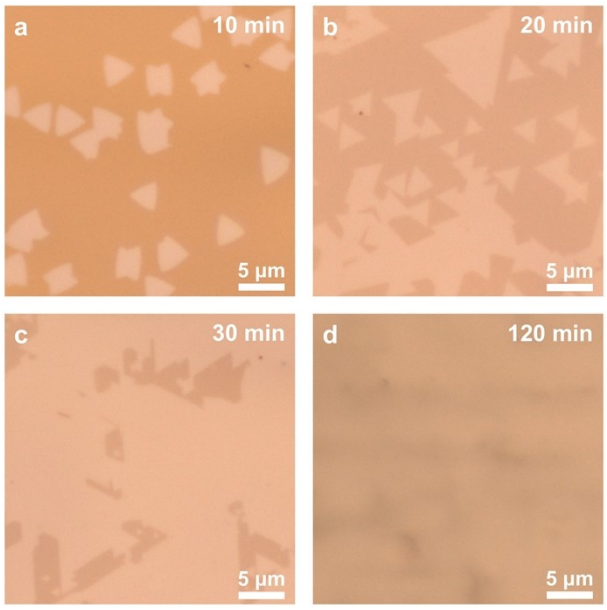

Figure S8. Optical images of monolayer h-BN samples grown by CVD for 10 min (a), 20 min (b), 30 min (c) and 120 min (d), respectively.

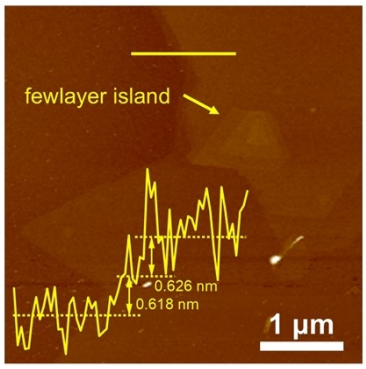

Figure S9. Few-layer h-BN samples can be obtained when using h-BN powders with partical size below 150 nm (99.9% purity, particle size <150 nm, Adamas).

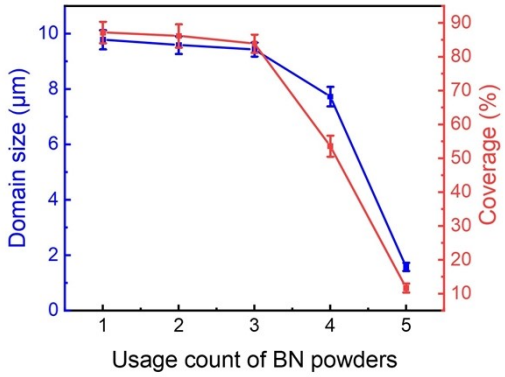

Figure S10. Domain size and coverage of monolayer h-BN samples grown on Cu substrates as a function of the usage count of the h-BN powders. Domain size and coverage of monolayer h-BN samples maintain the same level at the first three times, and decrease considerably starting from the fourth time, which means that the precursor, h-BN powder, can be used several times to growth 2D h-BN samples for further cost savings.

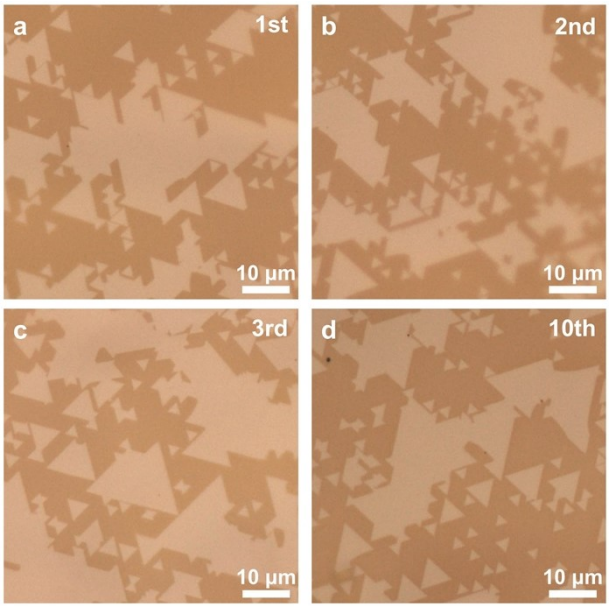

Figure S11. Optical images of monolayer h-BN samples grown on the same Cu substrate for 1st time (a), 2nd time (b), 3rd time (c) and 10th time (d).

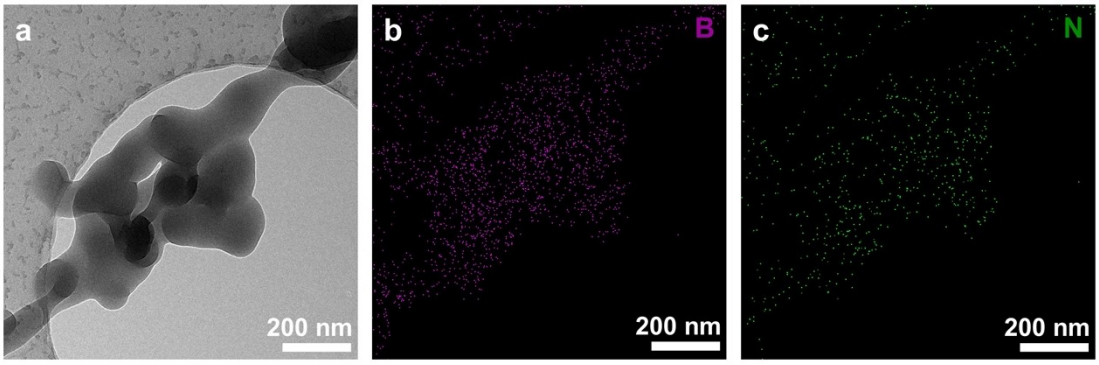

Figure S12. Low-magnification TEM image (a) of part of a free-standing 3D h-BN foam and its corresponding elemental mappings of B (b) and N (c).

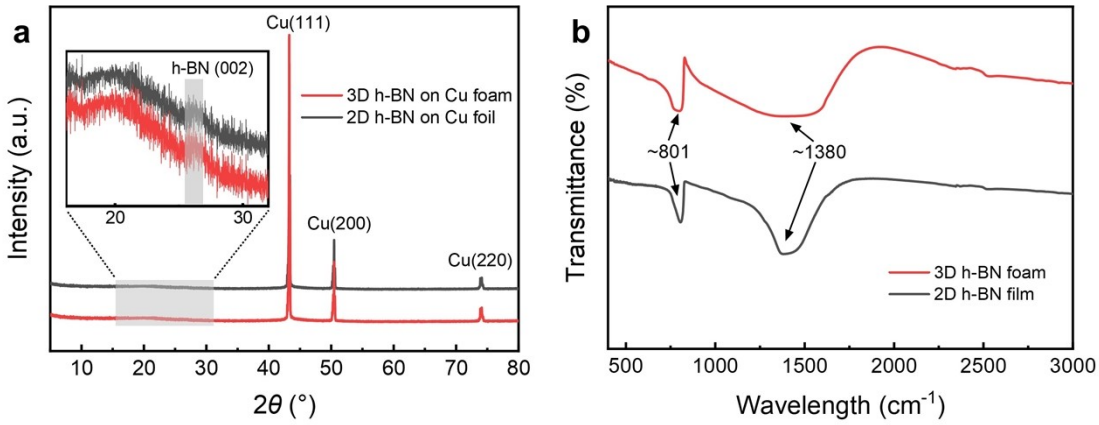

Figure S13 a) XRD patterns of 2D h-BN and 3D h-BN samples grown on Cu foil and Cu foam, respectively. The inset shows the weak (002) peak of h-BN. The XRD patterns of h-BN and copper refer to PDF card #01-073-2095 and #00-004-0836, respectively. b) FTIR spectra of 2D h-BN film and 3D h-BN foam.

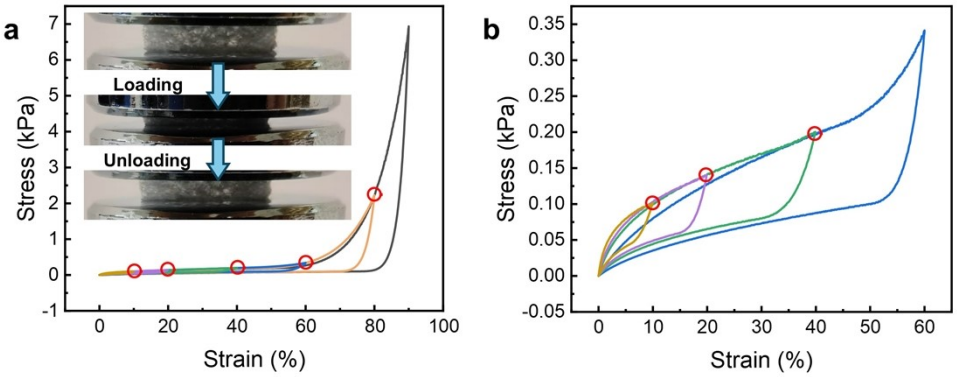

Figure S14. a) Stress-strain curves of BNF@PDMS composites during loading-unloading cycles in sequence of increasing strain amplitudes from 10% to 90%. The

inset shows the photographs of BNF@PDMS-21 undergoing a loading-unloading cycle. b) Enlarged curves of (a) from 10% to 80% strain amplitude.

Table S1. FWHM of 2D h-BN obtained with different synthesis methods.

Synthesis methods	Number of layers/Thickness	FWHM (cm^{-1})	Reference
Mechanical Exfoliation	1L	13.6	[1]
Liquid-Phase Exfoliation	2-3L	>20	[2]
	few layers	25.4	[3]
Traditional CVD	1L	14.5	[4]
	1L, 2L, few layers	15.6, 18.8, 26.1	[5]
	few layers	24.5	[6]
MOCVD	few layers	18-24	[7]
Green CVD	1L	16.2	This work

Table S2. The list of different densities of BNF@PDMS composites obtained by using different PDMS concentrations.

Foam	wt% of PDMS	ρ (mg/cm^3)	Designation
BNF	0	0.90 ± 0.05	BNF
BNF@PDMS	4	21.31 ± 1.74	BNF@PDMS-21
BNF@PDMS	6	34.54 ± 2.91	BNF@PDMS-35
BNF@PDMS	8	46.01 ± 3.03	BNF@PDMS-46

References

[1] Zeng, F.; Wang, R.; Wei, W.; Feng, Z.; Guo, Q.; Ren, Y.; Cui, G.; Zou, D.; Zhang, Z.; Liu, S.; et al. Stamped Production of Single-crystal Hexagonal Boron Nitride Monolayers on Various Insulating Substrates. *Nat. Commun.* **2023**, *14* (1), 6421. https://doi.org/10.1038/s41467-023-42270-x.

[2] Gonzalez Ortiz, D.; Pochat-Bohatier, C.; Cambedouzou, J.; Bechelany, M.; Miele, P. Exfoliation of Hexagonal Boron Nitride (h-BN) in Liquide Phase by Ion Intercalation. *Nanomater.* **2018**, *8* (9), 716. https://doi.org/10.3390/nano8090716.

[3] Zhang, Z.; Su, J.; Matias, A. S.; Gordon, M.; Liu, Y.-S.; Guo, J.; Song, C.; Dun, C.; Prendergast, D.; Somorjai, G. A.; Urban, J. J. Enhanced and Stabilized Hydrogen Production from Methanol by Ultrasmall Ni Nanoclusters Immobilized on Defect-rich h-BN Nanosheets. *Proc. Natl. Acad. Sci.* **2020**, *117* (47), 29442-29452. https://doi.org/10.1073/pnas.2015897117.

[4] Chen, T. A.; Chuu, C. P.; Tseng, C. C.; Wen, C. K.; Wong, H. S. P.; Pan, S. Y.; Li, R. T.; Chao, T. A.; Chueh, W. C.; Zhang, Y. F.; et al. Wafer-Scale Single-crystal Hexagonal Boron Nitride Monolayers on Cu (111). *Nature* **2020**, *579* (7798), 219-+. https://doi.org/10.1038/s41586-020-2009-2.

[5] Gao, Y.; Ren, W. C.; Ma, T.; Liu, Z. B.; Zhang, Y.; Liu, W. B.; Ma, L. P.; Ma, X. L.; Cheng, H. M. Repeated and Controlled Growth of Monolayer, Bilayer and Few-Layer Hexagonal Boron Nitride on Pt Foils. *ACS Nano* **2013**, *7* (6), 5199-5206. https://doi.org/10.1021/nn4009356.

[6] Bansal, A.; Hilse, M.; Huet, B.; Wang, K.; Kozhakhmetov, A.; Kim, J. H.; Bachu, S.; Alem, N.; Collazo, R.; Robinson, J. A.; et al. Substrate Modification during Chemical Vapor Deposition of hBN on Sapphire. *ACS Appl. Mater. Interfaces* **2021**, *13* (45), 54516-54526. https://doi.org/10.1021/acsami.1c14591.

[7] Jeong, H.; Kim, D. Y.; Kim, J.; Moon, S.; Han, N.; Lee, S. H.; Okello, O. F. N.; Song, K.; Choi, S.-Y.; Kim, J. K. Wafer-scale and Selective-area Growth of High-quality Hexagonal Boron Nitride on Ni(111) by Metal-organic Chemical Vapor Deposition. *Sci. Rep.* **2019**, *9* (1), 5736. https://doi.org/10.1038/s41598-019-42236-4.